Monthly Notices
of the
ROYAL ASTRONOMICAL SOCIETY

MNRAS **477,** 4707–4710 (2018) doi:10.1093/mnras/sty1093
Advance Access publication 2018 April 28

Erratum: The properties of radio galaxies and the effect of environment in large-scale structures at $z \sim 1$

by Lu Shen,[1]★ Neal A. Miller,[2] Brian C. Lemaux,[1] Adam R. Tomczak,[1] Lori M. Lubin,[1] Nicholas Rumbaugh,[3] Christopher D. Fassnacht,[1] Robert H. Becker,[1] Roy R. Gal,[4] Po-Feng. Wu[5] and Gordon Squires[6]

[1]*Physics Department, University of California, Davis, One Shields Avenue, Davis, CA 95616, USA*
[2]*Stevenson University, Department of Mathematics and Physics, 1525 Greenspring Valley Road, Stevenson, MD, 21153, USA*
[3]*National centre for Supercomputing Applications, University of Illinois, 1205 West Clark St., Urbana, IL 61801, USA*
[4]*University of Hawai'i, Institute for Astronomy, 2680 Woodlawn Drive, Honolulu, HI 96822, USA*
[5]*Max-Planck Institut für Astronomie, Königstuhl 17, D-69117, Heidelberg, Germany*
[6]*Spitzer Science centre, California Institute of Technology, M/S 220-6, 1200 E. California Blvd., Pasadena, CA, 91125, USA*

Key words: errata, addenda – galaxies: active – galaxies: clusters: general – galaxies: evolution – galaxies: groups: general – galaxies: star formation – radio continuum: galaxies.

This is an erratum to our paper 'The properties of radio galaxies and the effect of environment in large-scale structures at $z \sim 1$', which was published in MNRAS 472, 998–1022 (2017). Due to an error in our differential velocity formula when calculating global density (η), there are minor changes to the log(η) values in Tables 6, 7 and 8, and minor changes to the distributions of log(η) in Figs 8 and 9. We also corrected an issue in Table 6 where we previously listed η instead of log(η). We present the correct version of the tables and figures here. No results, analysis, or discussion are affected by this change. In addition, we note that two sentences need to be revised in Section 5.5.1.1. We repeat the paragraph which contains the sentences here and mark the changes in bold:

Table 6. Radio and X-ray cross-match.

Field	Radio ID	RA	Dec.	Radio power	X-ray ID[a]	X-ray Full Luminoisty[a]	log(η)[b]	Colour offset[c]	Type[d]
SC1604	502	241.0647	43.1713	23.28	0	6.269E+43	**−0.092**	0.038	Hybrid
SC1604	568	241.1076	43.2126	23.67	2	2.111E+43	**−0.106**	0.160	AGN
SC1604	681	241.1567	43.1494	24.30	6	6.175E+42	**−0.081**	0.038	AGN
RXJ1821	198	275.2819	68.3941	23.72	2	6.240E+42	**−0.206**	0.336	AGN
RXJ1821	237	275.3494	68.4424	23.15	0	7.728E+42	**−0.494**	0.375	SFG

[a]X-ray ID and Full band Luminosity adopted from Rumbaugh et al. (2016).
[b]log(η) parameter is described in Section 5.5.
[c]colouroffset parameter is explained in Section 5.1.
[d]The type of radio galaxy is based on our two-stage classification scheme.

We use the K-S test on the distributions of η between AGN and SFGs, and find a p-value of **∼0.08**, which implies that the AGN and SFGs do not share the same global environment distribution. Therefore, we conclude that AGN preferentially reside in the cluster/group environment, while SFGs generally avoid these regions. The K-S test between AGN and Hybrids, SFGs and Hybrids, and radio confirmed galaxies and spectroscopically-confirmed members are not conclusive (see Table 8, Table 8 in the published paper). We perform the same sampling algorithm here as in Section 5.1. We randomly select a sample from the combined AGN and SFG samples for 100 trials with the same number of galaxies in the Hybrid sub-class. In this way, we confirm that mixing AGN and SFGs can likely not produce the Hybrid distribution, as the mode of the p-values is **∼0.08**, when comparing these composite distributions with these of the Hybrids.

★ E-mail: lushen@ucdavis.edu

Table 7. Summary of average properties of the three radio populations.

Radio Type	$\langle Colour \rangle^a$	Colour Offset^b	$\log(\langle M_*/\mathrm{M}_\odot \rangle)^c$	$\log(\langle \eta \rangle)^d$	$\log(\langle 1+\delta_{\rm gal} \rangle)^e$	$\log(\langle L_{1.4\,\rm GHz} \rangle)$
AGN	4.62	0.10	11.16 ± 0.03	**−0.59**	0.67	24.01 ± 0.05
Hybrid	3.38	−0.74	10.74 ± 0.07	**−0.47**	0.58	23.21 ± 0.02
SFG	3.36	−0.71	10.95 ± 0.03	**−0.44**	0.48	23.21 ± 0.02

[a]Median value of Rest-frame $M_{NUV} - M_r$;
[b]Median value of colour offset parameter, derived in Section 5.1;
[c]With standard error of the median listed;
[d]$\eta = R_{proj}/R_{200} \times |\Delta_v|/\sigma_v$, see explanation in Section 5.5;
[e]See explanation on $\log(1 + \delta_{gal})$ in Section 5.5.

Table 8. Summary of *p*-values from K-S test.

Sample-sample type^a	Colour^b	Colour Offset^c	$\log(\langle M_*/\mathrm{M}_\odot \rangle)$	$\log(\langle \eta \rangle)^d$	$\log(\langle 1+\delta_{\rm gal} \rangle)^e$	$\log(\langle L_{1.4\,\rm GHz} \rangle)$
AGN-Hybrid	10^{-5}	10^{-6}	10^{-3}	**0.65**	0.10	10^{-11}
AGN-SFG	10^{-8}	10^{-6}	0.01	**0.08**	0.24	10^{-9}
Hybrid-SFG	0.18	0.09	0.05	**0.63**	0.91	0.93
Hybrid-Mixed^f	10^{-6}	0.02	10^{-4}	**0.08**	0.08	10^{-4}
Radio-Spec	0.004	0.006	10^{-14}	**0.31**	0.15	–

[a]Two compared galaxy samples.
[b]Rest-frame $M_{NUV} - M_r$;
[c]Colour offset parameter, derived in Section 5.1;
[d]$\eta = R_{proj}/R_{200} \times |\Delta_v|/\sigma_v$, see explanation in Section 5.5;
[e]See explanation on $\log(1 + \delta_{gal})$ in Section 5.5.
[f]A sample of mixture of AGN and SFGs, drawn with the same number of galaxies in the Hybrid population from AGN and SFG population for 100 trials, allowing the relative number of AGN and SFG to vary in each draw.

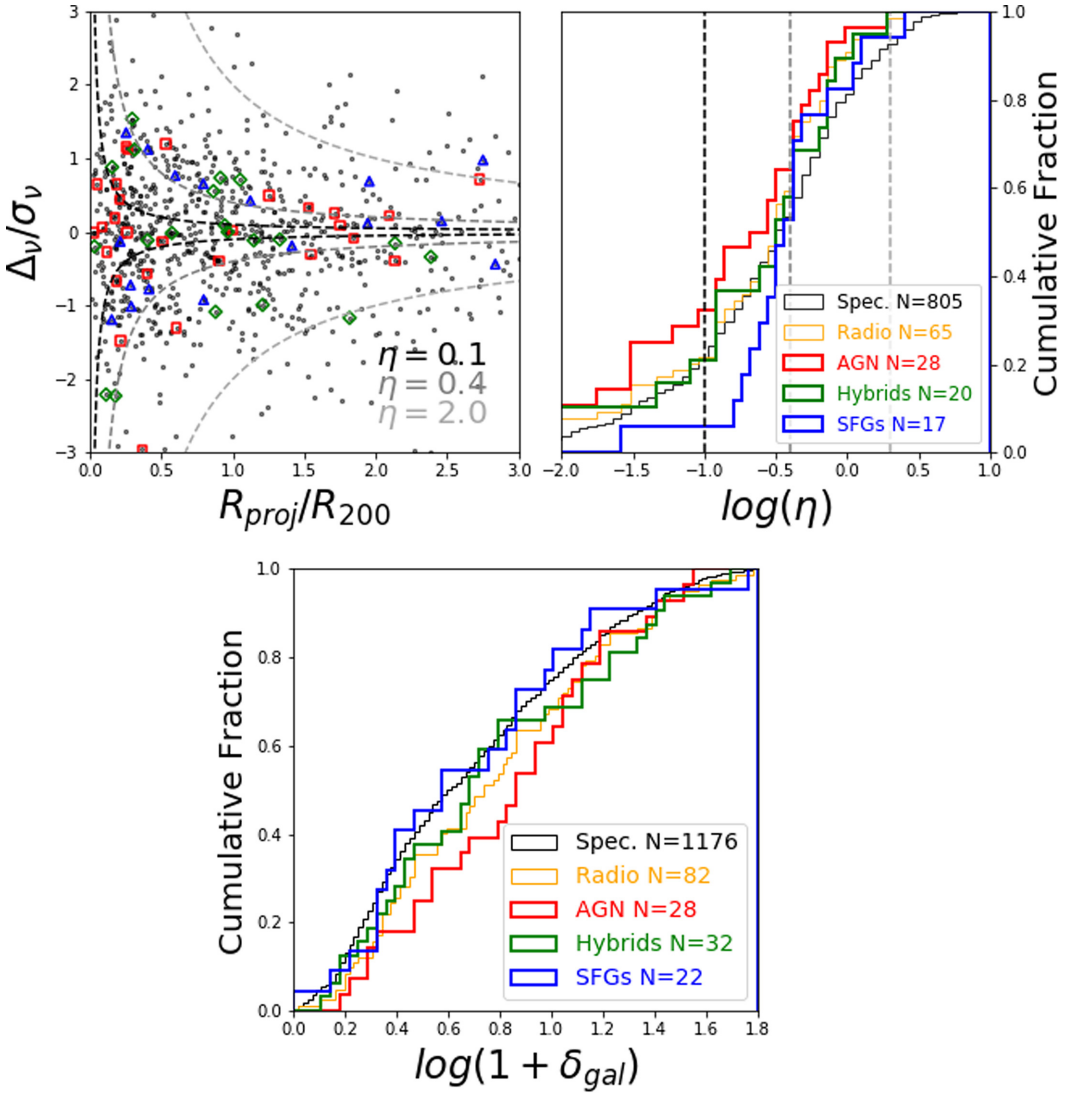

Figure 8. *Top left*: R_{proj}/R_{200} versus $|\Delta_v|/\sigma_v$ phase space diagram for spectroscopically-confirmed members (grey dots) and three radio populations (marked by open coloured squares). Three lines of constant η are displayed as well. *Top right*: CDFs of η. The red, green and blue histogram correspond to AGN, Hybrid and SFG population. The brown thin line represent the distribution of the overall radio sample, and the black line represents the distribution of spectroscopically-confirmed members. The number of galaxies in each class in both plots is displayed after their label. Three lines of constant η are displayed with same colour in the top panel. *Bottom*: CDFs of overdensity, on radio sub-classes, the overall radio and spectroscopically-confirmed samples. The colour convention is the same as the top right panel.

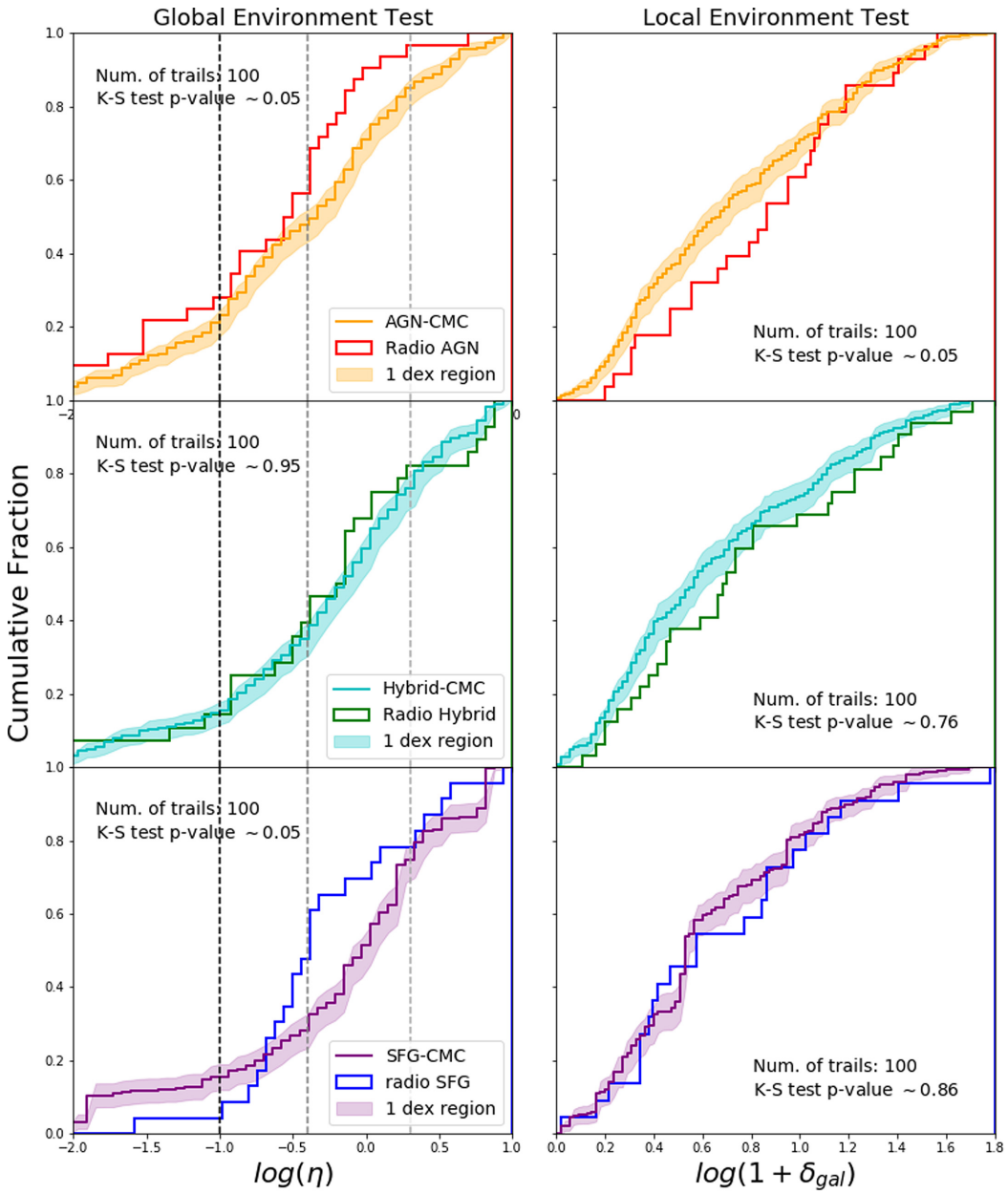

Figure 9. Global and local environment Cumulative Distribution histogram (CDF) on the radio sub-classes and their CMC sample. *Left*: CDF of $\eta = R_{proj}/R_{200} \times |\Delta_v|/\sigma_v$, for the three radio sub-classes and their CMC samples are plotted in the three panel, AGN (top), Hybrid (Middle), and SFG (Bottom), along with a 1σ shaded region on the mean of 100 re-samples. *Right*: CDF of $\log(1 + \delta_{gal})$, for the three radio sub-classes (colour depends on their radio type) and their CMC samples are plotted in the three panel, along with a 1σ shaded region on the mean of 100 re-samples. Three lines of constant $\eta =$ 0.1, 0.4, 2.0 are displayed as well

This paper has been typeset from a TEX/LATEX file prepared by the author..